Plastic-damage analysis of reinforced concrete frames

J. Faleiro, S. Oller and A.H. Barbat

CIMNE (International Center for Numerical Methods in Engineering), Barcelona, Spain, and Escuela Técnica Superior de Ingenieros de Caminos, Canales y Puertos, Technical University of Catolonia, Barcelona, Spain

Abstract

Purpose – The purpose of this paper is to develop an improved analytical model for predicting the damage response of multi-storey reinforced concrete frames modelled as an elastic beam-column with two inelastic hinges at its ends.

Design/methodology/approach – The damage is evaluated in the hinges, using the concentrated damage concepts and a new member damage evaluation method for frame members, which leads to a meaningful global damage index of the structure. A numerical procedure for predicting the damage indices of the structures using matrix structural analysis, plastic theory and continuum damage model is also developed. The method is adequate for the prediction of the failure mechanisms.

Findings – Using the proposed framework numerical examples are finally included. From the obtained results, the advantages and limitation of the proposed model are observed.

Originality/value – The numeric model presented is useful to solve multi-storey reinforced concrete frames using an inexpensive procedure that combines structural finite elements (beams) of low execution cost, with the moment-curvature constitutive models deriving from classic stress-strain ones. The proposed techniques give an inexpensive and reliability procedure to model the frame structures.

Keywords Reinforced concrete, Construction engineering, Structural analysis, Modelling

Paper type Research paper

1. Introduction

The constitutive models based on the continuum damage mechanics and the development of the numerical techniques enables to retake existing structural models and improve their capacity of evaluating the global damage state of reinforced concrete building. Plastic theory can be used as mathematical framework to treat permanent strains. However, in particular geomaterials, such as concrete, permanent strains are caused by microcracking, what leads to permanent stiffness degradation. In those cases, the plasticity theory itself is not satisfactory to represent the stiffness degradation, and therefore it is necessary to use another tool, the continuum damage mechanics.

Using the works of Kachanov (1958), continuum damage mechanics became one of the most studied subjects in solids mechanics. The main idea is defining a new damage internal variable which describes the evolution of microcracks and microvoids and their influence on the behaviour of the material. This simple and general idea has been used for modelling, until the local fracture, most of the construction materials. Initially introduced for metals, the continuum damage mechanics was later adapted to materials such as concrete (Oller, 2001). Currently, there are some models in which plasticity and damage are coupled (Simo and Ju, 1987; Oñate *et al.*, 1988; Luccioni *et al.*, 1995). This approach has the advantage of allowing the development of constitutive independent laws which simulate materials in which the plastic deformation is not significant, as in the case of concrete, ceramic and ceramic composites.

Nowadays, continuum mechanics is still not the most suitable analysis framework for certain civil engineering structures, like framed structures, which are usually

modelled by means of bar elements, while continuum mechanics is used mostly in the case of finite element (FE) models of the structure. Perhaps the main inconvenience in the use of finites elements consists in the fact that the most of the results obtained will be useless or of little practical utility for the structural designer (Salomón *et al.*, 1999; Mata *et al.*, 2007a, b). In this article we use the computational advantages of the matrix formulation for framed building structures, together with the complexity of the plastic-damage constitutive models.

Nonetheless, plasticity theory has been successfully adapted to frame analysis using the concept of lumped plasticity models, in which it is assumed that plastic effects can be concentrated at special locations called plastic hinges. This approach can be justified since in frame analysis the deformation is usually concentrated at or very near the end of the beams, and these are the only results of the frames analysis usually used by the structural designer.

Using the lumped plasticity model, Cipolina *et al.* (1995), Flórez-López (1993, 1995, 1999) and Oller and Barbat (2005) adapted the damage models to frame analysis in which the damage is concentrated on plastic hinges, developing thus a concentrated damage model. A value of the damage concentrated at the hinge equal to 1 reflects complete loss of strength while a value 0 means no damage. However, this method has the inconvenience that only refers to the damage at the hinge, and do not take into account the effect of cumulative plastic deformations under cyclic loading. Another inconvenience is that once the concentrated damage index is located at the end of the frame member, it is not possible to determine the real damage state of the member.

Starting from the method proposed by Hanganu *et al.* (2002), this article develops a global damage evaluation method based on continuum mechanics principles in which the label "member damage" will be applied only to damage indices describing the state of frame member while the "global" damage indices will refers to state of whole structure (Martinez *et al.*, 2008; Mata *et al.*, 2008a, b). Both member and global damage indices considered herein are independent from the constitutive models chosen for the structural material.

This feature converts the proposed member and global damage indices into a powerful general tool for the structural behaviour assessment. Moreover, it is applicable directly to both static and dynamic analyses and can be used to estimate the damage produced by seismic actions in reinforced concrete building structures.

This paper will describe the procedure to use plastic-damage models in frame structures analysis, with application to reinforced concrete structures, in accordance with the classic theories of continuum damage mechanics and of plasticity. These theories will give support to the implementation of the member and global damage indices. What distinguishes this work from others is the fact that the complete plastic-damage constitutive model, as well as the global damage, is here implemented into a frame analysis algorithm, which is briefly outlined. Finally, the method is validated through various analyses of framed structures.

2. Basic definitions
Let us consider a plane frame with b elements, connected into n nodes. The displacement of the structure is studied during a time interval $[0,T]$. At time $t = 0$, the state of the structure is denoted as "initial or undeformed configuration". The configuration of the structure will be called "deformed" for any $t > 0$. As a reference, we will consider a couple of orthogonal coordinate axes X and Y to define the

position of each node in any configuration. During the deformation of the structure, this coordinate system is assumed to be stationary.

Beams or columns extremities define the frame elements, where joints i and joint j indicate an element. Conventionally, the direction of each element is defined by the $i - j$ nodes. Each joint has three degrees of freedom. For example, the generalized nodal displacement in a node i can be defined as $\{\mathbf{u_i}\}^{\mathrm{T}} = \{q_1 \quad q_2 \quad q_3\}$, where q_1, q_2 and q_3 indicate the node displacement in the directions X and Y, and the node rotation with respect to the initial configuration, respectively. In this article $\{\bullet\}$ indicates a column matrix and $[\bullet]$ indicates a quadratic matrix.

For each element b, the generalized displacement vector for nodes $i - j$ can be defined as $\{\mathbf{q}_b\}^{\mathrm{T}} = \{\mathbf{u}_\mathrm{i}^{\mathrm{T}} \quad \mathbf{u}_\mathrm{j}^{\mathrm{T}}\} = \{q_1 \quad q_3 \quad q_2 \quad q_4 \quad q_5 \quad q_6\}$ and the global displacement $\mathbf{U}$ of the structure is

$$\{\mathbf{U}\}^{\mathrm{T}} = \{\mathbf{u}_1^{\mathrm{T}} \quad \mathbf{u}_2^{\mathrm{T}} \quad \cdots \quad \mathbf{u}_n^{\mathrm{T}}\} \tag{1}$$

The generalized deformations $\mathbf{\Phi}_b$ of the beam b can be defined as

$$\{\mathbf{\Phi}_b\}^{\mathrm{T}} = \{\phi_i \quad \phi_j \quad \delta\} \tag{2}$$

where ϕ_i and ϕ_j indicate rotations of the member at the ends i and j, respectively, and δ is its elongation. The generalized deformations $\mathbf{\Phi}_b$ can be expressed in terms of the global displacement $\mathbf{U}$ by

$$\mathbf{\Phi}_b = \mathbf{B}_b \cdot \mathbf{U} \tag{3}$$

where $\mathbf{B}_b$ is the global displacement transformation matrix.

The generalized "effective" stress vector of the frame element b is defined as

$$\{\boldsymbol{M}_b\}^{\mathrm{T}} = \{m_i \quad m_j \quad n\} \tag{4}$$

which contains the final forces of the member, where m_i and m_j are the moments at the ends of the member and n indicates the axial force. The internal force is the sum of all generalized effective stress $\boldsymbol{M}_b$

$$\mathbf{F}_{int} = \sum_{b=1}^{3nth} \mathbf{B}_b^{\mathrm{T}} \cdot \boldsymbol{M}_b \tag{5}$$

The structure is subjected to concentrated forces and moments acting only on the nodes, grouped into a vector $\mathbf{F}_{ext}$

$$\{\mathbf{F}_{ext}\}^{\mathrm{T}} = \{ \underbrace{f_1, f_2, f_3}_{\text{forces on node } 1} \quad \cdots \quad \underbrace{f_{3n-2}, f_{3n-1}, f_{3n}}_{\text{forces on node } n}\} \tag{6}$$

Using now the expressions of the inertial and internal forces, the quasi-static equilibrium of the nodes is expressed as

$$\mathbf{F}_{ext} - \mathbf{F}_{int} = 0 \tag{7}$$

The relation between generalized stress and the history of deformations can be expressed as follows:

$$\boldsymbol{M}_b = \mathbf{S}_b^e(\boldsymbol{\Phi}_b) \cdot \boldsymbol{\Phi}_b \quad \text{or} \quad \boldsymbol{\Phi}_b = \boldsymbol{\mathcal{F}}_b^e(\boldsymbol{M}_b) \cdot \boldsymbol{M}_b \tag{8}$$

where $\mathbf{S}_b^e(\boldsymbol{\Phi}_b)$ and $\boldsymbol{\mathcal{F}}_b^e(\mathbf{M}_b)$ indicate the local elastic stiffness and flexibility matrices, respectively. They are defined according to the deformed configuration of the member.

In the case of small deformations, the elastic stiffness and flexibility matrices remain constant. In this context, Equation (8) can be rewritten as

$$\boldsymbol{M}_b = \mathbf{S}_b^e \cdot \boldsymbol{\Phi}_b \quad \text{or} \quad \boldsymbol{\Phi}_b = \boldsymbol{\mathcal{F}}_b^e \cdot \boldsymbol{M}_b \tag{9}$$

with $\mathbf{S}_b^e = \boldsymbol{\mathcal{F}}_b^{e^{-1}}$ being the stiffness elastic matrix. Inserting Equation (9) into (7) and expanding the expression as a function of displacements

$$\underbrace{\left(\sum_{b=1}^{n\ elements} \mathbf{B}_b^{\mathrm{T}} : \mathbf{S}_b : \mathbf{B}_b \right)}_{Internal\ Force} : \mathbf{U} = \mathbf{F}_{ext} \tag{10}$$

$\mathbf{K}^e = \sum \mathbf{B}_b^{\mathrm{T}} : \mathbf{S}_b^e : \mathbf{B}_b$ is the global stiffness matrix.

3. Concentrated plasticity approach for frame members
For many reinforced concrete cross-sectional shapes, the spread of plasticity starting from the ends of the members along the length is not very significant, and the deformation is concentrated at or very near the cross-sections of the ends (Deierlein *et al.*, 2001). Therefore, we will assume that all the plasticity is concentrated at the end cross-sections. We also assume that the yielding of an end cross-section is sudden, rather than gradual or fibre-by-fibre, and that the material behaves in a perfectly elastic plastic manner.

3.1 Lumped plasticity model
A constitutive equation can be obtained relating the generalized stress $\boldsymbol{M}_b$ with the generalized deformations $\boldsymbol{\Phi}_b$ by using the lumped dissipation model, considering plasticity, hardening or any other energy dissipation. Energy dissipation is assumed to be concentrated only at the hinges, while beam-column behaviour always remains elastic. With these concepts, we can express the member deformations as

$$\boldsymbol{\Phi}_b = \underbrace{\boldsymbol{\mathcal{F}}_b^e \cdot \boldsymbol{M}_b}_{\boldsymbol{\Phi}^e} + \boldsymbol{\Phi}_b^p \tag{11}$$

The term $\boldsymbol{\mathcal{F}}_b^e : \boldsymbol{M}_b = \boldsymbol{\Phi}^e$ corresponds to the beam-column elastic deformations, while $\boldsymbol{\Phi}_b^p$ is called "plastic hinge deformations"

$$\{\boldsymbol{\Phi}_b^p\}^{\mathrm{T}} = \left\{ \phi_i^p \quad \phi_j^p \quad \delta^p \right\} \tag{12}$$

where ϕ_i^p and ϕ_j^p represent the plastic rotations of the member at the ends i and j, respectively, and δ^p is its plastic elongation. Using the generalized stress $\boldsymbol{M}_b$ from Equation (11), we will obtain (Cipolina *et al.*, 1995; Faleiro *et al.*, 2005)

$$M_b = S_b^e \cdot (\mathbf{\Phi}_b - \mathbf{\Phi}_b^p) \tag{13}$$

Equation (13) assumes that plastic hinges produced when the load on structure increases until the structure becomes unstable (or a mechanism) due to the development of various plastic hinges. Once a mechanism is formed, the structure continues to deform until the final instability is detected by the singularity of the global stiffness matrix.

3.2 Internal variable evolution laws and plastic functions

For the internal variables defined in Equation (12), the plastic deformation evolution laws for each hinged ends i and j of the beam subjected to bending, the plastic deformation evolution laws are (Cipolina *et al.*, 1995):

$$\dot{\phi}_i^p = \dot{\lambda}_i^p \frac{\partial f_i}{\partial m_i}, \quad \dot{\phi}_j^p = \dot{\lambda}_j^p \frac{\partial f_j}{\partial m_j} \tag{14}$$

while for the case of axial mechanism, the plastic deformation evolution law is (Cipolina *et al.*, 1995):

$$\dot{\delta}^p = \dot{\lambda}_i^p \frac{\partial f_i}{\partial n} + \dot{\lambda}_j^p \frac{\partial f_j}{\partial n} \tag{15}$$

where $f_i \leq 0$ and $f_j \leq 0$ are the yield functions of hinges i and j, respectively. These functions depend on the generalized stress M_b and also depend on the internal variables and plastic multipliers $\dot{\lambda}_i^p$ and $\dot{\lambda}_j^p$. The plastic multipliers according to the Kuhn-Tucker conditions are:

$$\text{No plasticity} \begin{cases} \dot{\lambda}_i^p = 0 & \text{if } f_i < 0 \quad \text{or} \quad \dot{\lambda}_i^p f_i = 0 \\ \dot{\lambda}_j^p = 0 & \text{if } f_j < 0 \quad \text{or} \quad \dot{\lambda}_j^p f_j = 0 \end{cases}$$
$$\text{Plasticity state} \begin{cases} \dot{\lambda}_i^p > 0 & \text{if } f_i = 0 \quad \text{and} \quad \dot{\lambda}_i^p f_i = 0 \\ \dot{\lambda}_j^p > 0 & \text{if } f_j = 0 \quad \text{and} \quad \dot{\lambda}_j^p f_j = 0 \end{cases} \tag{16}$$

To plastic multiplier strictly positive, we will consider that the plastic deformation is "active"; otherwise it will be called "passive".

3.2.1 Plastic functions. The plastic inner variables evolution laws are activated when the yield criterion is verified (see Equation (16)). This criterion used for the end of beam hinges is a function of the bending moment at each of the end cross-sections and of the axial force along the beam (Cipolina *et al.*, 1995; Argyris *et al.*, 1982)

$$f_i = \frac{|m_i|}{m_p(\phi_i^p)} + \left(\frac{n}{n_p(\delta^p)}\right)^2 - \alpha = 0 \quad f_j = \frac{|m_j|}{m_p(\phi_j^p)} + \left(\frac{n}{n_p(\delta^p)}\right)^2 - \alpha = 0 \tag{17}$$

where m_p is the yield moment or plastic moment, n_p is the yield axial force and α is an additional hardening function of the material.

Despite the fact that the yield surface is the same for the hinges i and j, the plastic multipliers are independent of each other. Other yield functions can be formulated to

describe the complete yielding of the cross-section, the residual stress effects or the behaviour of different materials, as proposed in Deierlein *et al.* (2001).

3.2.2 Plastic return-mapping corrector. In order to fulfil with the yield criterion imposed by Equation (17), a similar procedure to return-mapping algorithm is used, but in this case expressed in terms of moments and axial forces. The final moments are

$$m_i = m_i^{trial} - \dot{\lambda}_i^p \cdot \mathbf{S}_b : \frac{\partial f_i}{\partial m_i^{trial}}$$
$$m_j = m_j^{trial} - \dot{\lambda}_j^p \cdot \mathbf{S}_b : \frac{\partial f_j}{\partial m_j^{trial}} \tag{18}$$

where $\dot{\lambda}_i^p$ and $\dot{\lambda}_j^p$ are the plastic multipliers and $\partial f_i/\partial m_i^{trial}$ and $\partial f_j/\partial m_j^{trial}$ are the plastic yield vectors, defined according to of the moments outside the yield surface. The moments m_i^{trial} and m_j^{trial} are the initial moments in the time step.

4. Continuous damage model at local level

Some basic concepts of continuum mechanics, necessary for the subsequent development of the concentrated damage concepts, are reviewed herein (Simo and Ju, 1987). Here we applied the damage effect on the properties of the elastic material while its influence in the plasticity parameters has been neglected. Physically, the degradation of the material properties is the result of the initiation, growth and coalescence of microcracks or microvoids. Within the context of continuum mechanics, one can model this process by introducing an internal damage variable that can be a scalar or a tensorial quantity. Let us consider $\mathbf{A}$, a fourth-order tensor, which characterizes the state of damage and transforms the effective stress tensor, $\bar{\boldsymbol{\sigma}}$, into the homogenized one, $\boldsymbol{\sigma}$, or vice versa:

$$\boldsymbol{\sigma} = \mathbf{A} : \bar{\boldsymbol{\sigma}} \tag{19}$$

For the isotropic damage case, the mechanical behaviour of microcracks or microvoids is independent on their orientation and depends only on a scalar variable d. For this reason, $\mathbf{A}$ will simply reduce to $\mathbf{A} = (1 - d)\mathbf{I}$, where $\mathbf{I}$ is a rank four identity tensor; thus, Equation (19) becomes

$$\boldsymbol{\sigma} = (1 - d)\bar{\boldsymbol{\sigma}} \tag{20}$$

where d is the scalar damage internal variable, $\boldsymbol{\sigma}$ the Cauchy stress tensor and $\bar{\boldsymbol{\sigma}}$ is the effective stress tensor, both at time t. Here, $d \in (0, 1]$ is a given constant. The coefficient $1 - d$ dividing the stress tensor in Equation (20) is a *reduction factor* associated with the amount of damage in the material, initially introduced by Kachanov (1958). The value $d = 0$ corresponds to the undamaged state, whereas a value $d = 1$ corresponds to a complete damaged state defining a local rupture. Another possible interpretation is that, physically, the damage parameter d is the ratio of the damage cross-section area to the total cross-section area.

4.1 Flexibility matrix of damaged member

Consider that the concentrated damage of the frame element b is defined as (Flórez-López,1995; Oller *et al.*, 1996a, b; Luccioni and Oller, 1996; Faleiro *et al.*, 2008)

$$\{\mathbf{D}^b\}^T = \{d_i \quad d_j \quad d_\delta\} \tag{21}$$

where d_i and d_j are a measure of the bending concentrated damage of hinges i and j, respectively, and d_δ indicates the measure of axial damage of the member. These variables can take values between zero (no damage) and one (completely damaged). In the same way as in the case of the plasticity, all the bending concentrated damage parameters are concentrated at the nodes. Supposing the existence of a flexibility bending matrix of a damaged member $[\mathcal{F}_b^d]_{\text{bend}}$ we have (Faleiro *et al.*, 2005, 2008)

$$[\mathbf{\Phi}_b]_{\text{bend}} = [\mathcal{F}_b^d]_{\text{bend}} \cdot [\mathbf{M}_b]_{\text{bend}} \Rightarrow \begin{Bmatrix} \phi_i \\ \phi_j \end{Bmatrix}_{\text{bend}} = \begin{bmatrix} f_{ii} & f_{ij} \\ f_{ji} & f_{jj} \end{bmatrix}_{\text{bend}} \begin{Bmatrix} m_i \\ m_j \end{Bmatrix}_{\text{bend}} \tag{22}$$

$$[\mathcal{F}_b^d]_{\text{bend}} = \frac{L}{6EI} \begin{bmatrix} \dfrac{2}{(1-d_i)} & -1 \\ -1 & \dfrac{2}{(1-d_j)} \end{bmatrix}_b \tag{23}$$

The inverse of $[\mathcal{F}_b^d]_{\text{bend}}$ is the stiffness bending matrix of a damaged member $[\mathbf{S}_b^d]_{\text{bend}} = [\mathcal{F}_b^d]_{\text{bend}}^{-1}$. If we also include the influence of axial mechanism in an uncoupled form, and redefine the stiffness matrix as a function of concentrated damage vector $\mathbf{D}^b$ for an element b, in small displacements we have (Faleiro *et al.*, 2008)

$$\begin{aligned} \mathbf{S}_b^d(\mathbf{D}^b) &= \begin{bmatrix} \left[\mathbf{S}_b^d\right]_{\text{bend}} & \mathbf{0} \\ \mathbf{0} & \left[\mathbf{S}_b^d\right]_{\text{axial}} \end{bmatrix} \\ &= k \begin{bmatrix} \begin{bmatrix} 12(1-d_i) & 6(1-d_i)(1-d_j) \\ 6(1-d_i)(1-d_j) & 12(1-d_j) \end{bmatrix}_{\text{bend}} & 0 \\ 0 & \\ 0 & 0 & \left[\dfrac{EA(1-d_\delta)}{kL}\right]_{\text{axial}} \end{bmatrix} \end{aligned} \tag{24}$$

where $k = 1/(4 - (1-d_i)(1-d_j))(EI/L)$. In the particular case when $\mathbf{D}^b$ trends to zero, $\mathbf{S}_b^d$ reduces to the standard stiffness elastic matrix $\mathbf{S}_b^d(\mathbf{D}^b = \mathbf{0}) \Rightarrow \mathbf{S}_b^e$.

4.2 Damage evolution law

In order to apply the continuum damage mechanics concepts to the framed structures analysis, it is necessary to express the damage variable evolution as a function of the deformations at the hinges i and j, as well as of the deformation due to the elongation δ. In addition, another necessary condition is that the evolutions of the damage variable should be independent of each other.

4.2.1 Free energy potential. Defining the free energy $\Psi_\varepsilon = 1/2\boldsymbol{\varepsilon} : \mathbf{C} : \boldsymbol{\varepsilon}$ (Malvern, 1969), where $\mathbf{C}$ is the constitutive tensor, $\boldsymbol{\varepsilon}$ is the total strain in each point of the solid,

and redefining it for a frame element b as a function of generalized strains $\mathbf{\Phi}_b$ and the stiffness matrix $\mathbf{S}_b$, we obtain the free energy potential as (see Faleiro *et al.*, 2008)

$$\Psi(\mathbf{\Phi}_b) = \Psi^0 = \frac{1}{2}\mathbf{\Phi}_b \cdot \mathbf{S}_b \cdot \mathbf{\Phi}_b \tag{25}$$

By rewriting (25) in terms of the rotations ϕ_i and ϕ_j at the ends of the element, as well as of the elongation δ, we obtain

$$\Psi^0 = \frac{1}{2}\left(4\frac{EI}{L}\phi_i + 2\frac{EI}{L}\phi_j\right)\phi_i + \frac{1}{2}\left(4\frac{EI}{L}\phi_j + 2\frac{EI}{L}\phi_i\right)\phi_j + \frac{1}{2}\frac{EA}{L}\delta^2 \tag{26}$$

In Equation (26) we observe that the free energy potential is the sum of the energies due to the rotations at the nodes i and j and to the elongation δ, in such a way that the free energy potential can be redefined as $\Psi^0 = \Psi_i^0 + \Psi_j^0 + \Psi_\delta^0$ where

$$\Psi_i^0 = \frac{1}{2}\left(4\frac{EI}{L}\phi_i + 2\frac{EI}{L}\phi_j\right)\phi_i, \quad \Psi_j^0 = \frac{1}{2}\left(4\frac{EI}{L}\phi_j + 2\frac{EI}{L}\phi_i\right)\phi_j \quad \text{and} \quad \Psi_\delta^0 = \frac{1}{2}\frac{EA}{L}\delta^2 \tag{27}$$

Introducing now $m_i = 4(EI/L)\phi_i + 2(EI/L)\phi_j$, $m_j = 4(EI/L)\phi_j + 2(EI/L)\phi_i$ and $n = (EA/L)\delta$, we can express Ψ_i^0, Ψ_j^0 and Ψ_δ^0 in terms of the moments at the ends of the beam m_i and m_j and the axial force n as

$$\Psi_i^0 = \frac{1}{2}m_i\phi_i; \quad \Psi_j^0 = \frac{1}{2}m_j\phi_j; \quad \Psi_\delta^0 = \frac{1}{2}n\delta \tag{28}$$

4.2.2 Energy norm for the undamaged structure and damage evolution. The undamaged energy norm vector τ^b is defined in the same way as the free energy, that is, as a function of the rotations ϕ_i and ϕ_j at the ends of the element and by the elongation δ (Faleiro *et al.*, 2008)

$$\tau_k^b = \left[\sqrt{\mathbf{\Phi}_b \cdot \mathbf{S}_b \cdot \mathbf{\Phi}_b}\right]_k = \begin{cases} \tau_i^b = \sqrt{2\Psi_i^0} = \sqrt{\left(4\dfrac{EI}{L}\phi_i + 2\dfrac{EI}{L}\phi_j\right)\phi_i} \\[2mm] \tau_j^b = \sqrt{2\Psi_j^0} = \sqrt{\left(4\dfrac{EI}{L}\phi_j + 2\dfrac{EI}{L}\phi_i\right)\phi_j}; \quad \forall k \in (i,j,\delta) \\[2mm] \tau_\delta^b = \sqrt{2\Psi_\delta^0} = \sqrt{\dfrac{EA}{L}\delta^2} \end{cases} \tag{29}$$

We characterize the damage state of the frame elements by means of three different and independent damage criteria: two of them are applied in the hinges at each end of the beam (i and j) and the third one is used for the axial damage control along the beam. This independent axial damage criterion allows the control of the axial stiffness of the reinforced concrete beam when the bending damage is reached in the concrete but the

$$g_k(\tau_k^b, r_k^b)_t = \begin{cases} g_i(\tau_i^b, r_i^b)_t = (\tau_i^b)_t - (r_i^b)_t \leq 0 \\ g_j(\tau_j^b, r_j^b)_t = (\tau_j^b)_t - (r_j^b)_t \leq 0 \; ; \quad \forall k \in (i, j, \delta) \\ g_\delta(\tau_\delta^b, r_\delta^b)_t = (\tau_\delta^b)_t - (r_\delta^b)_t \leq 0 \end{cases} \tag{30}$$

Here, the subscript t refers to the value at current time $t \in \mathbb{R}_+$, r_i^b, r_j^b and r_δ^b are the damage thresholds at the current time for the rotations ϕ_i and ϕ_j and for the elongation δ, respectively. We consider a vector r_0, for $t = 0$, which denotes the initial damage threshold before applying any load, defined as

$$(r_k^b)_0 = \sqrt{(\mathbf{M}_b)_d \cdot \mathbf{S}_b^{-1} \cdot (\mathbf{M}_b)_d} = \begin{Bmatrix} (r_i^b)_0 \\ (r_j^b)_0 \\ (r_\delta^b)_0 \end{Bmatrix} \Rightarrow \begin{cases} (r_i^b)_0 = (r_j^b)_0 = \sqrt{\dfrac{L}{3EI} m_d^2} \\ (r_\delta^b)_0 = \sqrt{\dfrac{L}{EA} n_d^2} \end{cases} ; \quad \forall k \in (i, j, \delta)$$

$$\tag{31}$$

where m_d and n_d are the limit values of the bending moment and axial force, respectively. The vector r_0 is a characteristic property of the material of the beam, in such a way that we must have $(r_k^b)_t \geq (r_k^b)_0, \forall k \in (i, j, \delta)$. Equation (30) states that damage in the element is initiated when the *energy norm* vector τ^b exceeds the initial damage threshold r_0. For the isotropic case, we define the evolution of the damage variables by

$$\dot{\mathbf{D}}_t^b = \dot{\lambda}^d H(\tau_k^b, \mathbf{D}_k^b)_t = \begin{cases} \dot{d}_i = \dot{\lambda}_i^d(\tau_i^b, d_i)_t \\ \dot{d}_j = \dot{\lambda}_j^d(\tau_j^b, d_j)_t \; ; \\ \dot{d}_\delta = \dot{\lambda}_\delta^d(\tau_\delta^b, d_\delta)_t \end{cases} \quad (\dot{r}_k^b)_t = \dot{\lambda}_t^d = \begin{cases} (\dot{r}_i^b)_t = \dot{\lambda}_i^d \\ (\dot{r}_j^b)_t = \dot{\lambda}_j^d \\ (\dot{r}_\delta^b)_t = \dot{\lambda}_\delta^d \end{cases} \tag{32}$$

where $\dot{\lambda}_i^d \geq 0$, $\dot{\lambda}_j^d \geq 0$ and $\dot{\lambda}_\delta^d \geq 0$ are *damage consistency* parameters that define the damage loading/unloading conditions according to the Kuhn-Tucker conditions

$$\text{Damage state} \begin{cases} \dot{\lambda}_i^d > 0 \quad \text{if } g_i(\tau_i^b, r_i^b)_t = 0 \quad \text{and} \quad \dot{\lambda}_i^d g_i = 0 \\ \dot{\lambda}_j^d > 0 \quad \text{if } g_j(\tau_j^b, r_j^b)_t = 0 \quad \text{and} \quad \dot{\lambda}_j^d g_j = 0 \\ \dot{\lambda}_\delta^d > 0 \quad \text{if } g_\delta(\tau_\delta^b, r_\delta^b)_t = 0 \quad \text{and} \quad \dot{\lambda}_\delta^d g_\delta = 0 \end{cases} \tag{33}$$

Let us now analyse the concentrated damage evolution at hinge k. Conditions (33) are standard for problems involving unilateral constraint. If $g_k < 0$, the damage criterion is not satisfied and, according to condition $\dot{\lambda}_k = 0$, the damage rule (32) implies that $\dot{d}_k = 0$ and no further damage occurs. If, on the other hand, $\dot{\lambda}_k^d > 0$, further damage occurs and condition (33) now implies that $g_k = 0$. In this case, the value of $\dot{\lambda}_k$ can be determined by the damage consistency condition, i.e.

$$g_k(\tau_k^b, r_k^b)_t = \dot{g}_k(\dot{\tau}]_k^b, \dot{r}_k^b)_t = 0 \quad \Rightarrow \dot{\lambda}_k^d = (\dot{\tau}_k^b)_t \tag{34}$$

Finally, $(r_k^b)_t$ can be calculated by means of the expression $(r_k^b)_t = \max\{(r_k^b)_0,$ $\max_{s\in(0,t)}(\tau_k^b)_s\}$. By applying it to all parameters, we obtain

$$(r_k^b)_t = \max\left\{(r_k^b)_t, \max_{s\in(0,t)}(\tau_k^b)_s\right\} = \begin{cases} \max\{(r_i^b)_0, \max_{s\in(0,t)}(\tau_i^b)_s\} \\ \max\{(r_j^b)_0, \max_{s\in(0,t)}(\tau_j^b)_s\} \\ \max\{(r_\delta^b)_0, \max_{s\in(0,t)}(\tau_\delta^b)_s\} \end{cases} \tag{35}$$

If we now consider that $H((\tau_k^b)_t, \mathbf{D}_t^b)$ in condition (32) is independent on the vector $\mathbf{D}_t^b$ and we also assume the existence of a monotonic function G, such that $H(\tau_k^b)_t = \partial G(\tau_k^b)_t/\partial(\tau_k^b)_t$, the damage criterion defined in (30) can be rewritten as a function of G, i.e. at hinge k $g_k(\tau_k^b, r_k^b)_t = G(\tau_k^b)_t - G(r_k^b)_t \leq 0$. In this way, the flow rule (32) and loading/unloading conditions (33) become

$$\dot{\mathbf{D}}_t^b = \dot{\lambda}_k^d \frac{\partial G(\tau_k^b, r_k^b)_t}{\partial(\tau_k^b)_t} = \begin{cases} \dot{d}_i = \dot{\lambda}_i^d \dfrac{\partial G((\tau_i^b)_t, (r_i^b)_t)}{\partial(\tau_i^b)_t} \\ \dot{d}_j = \dot{\lambda}_j^d \dfrac{\partial G((\tau_j^b)_t, (r_j^b)_t)}{\partial(\tau_j^b)_t} \; ; \\ \dot{d}_\delta = \dot{\lambda}_\delta^d \dfrac{\partial G((\tau_\delta^b)_t, (r_\delta^b)_t)}{\partial(\tau_\delta^b)_t} \end{cases} \quad (\dot{r}_k^b)_t = \dot{\lambda}_k^d = \begin{cases} (\dot{r}_i^b)_t = \dot{\lambda}_i^d \\ (\dot{r}_j^b)_t = \dot{\lambda}_j^d \\ (\dot{r}_\delta^b)_t = \dot{\lambda}_\delta^d \end{cases}$$

$$\tag{36}$$

Carrying out the time integration of the rate concentrated damage vector, the result is an expression that indicates the evolution of the damage variables as

$$\mathbf{D}_t^b = G(\tau_k^b)_t = \begin{cases} G(\tau_i^b)_t = d_i \\ G(\tau_j^b)_t = d_j \; ; \quad \forall k \in (i,j,\delta) \\ G(\tau_\delta^b)_t = d_\delta \end{cases} \tag{37}$$

The scalar function $G(\cdot)$ defining the evolution of the damage variable must be monotonic in the range $0 \leq G(\cdot) \leq 1$ and can be defined according to the type of analysis. In our work, the expression of the exponential softening was used

$$G(\tau_k^b)_t = 1 - \frac{(\tau_k^b)_t}{(r_k^b)_0} e^{K_A\left(1-(r_k^b)_0/(\tau_k^b)_t\right)}; \quad \forall k \in (i,j,\delta) \tag{38}$$

where the energy norm vector is ranged $0 \leq (\tau_k^b)_t \leq (r_k^b)_0$ and is a parameter dependent on the fracture energy $K_A = K_A(G_f)$ (Oller, 2001; Barbat *et al.*, 1997; Lubliner *et al.*, 1989).

5. Plastic-damage model for reinforced concrete frames
Elastic damage or elastic plastic laws are not sufficient to represent the constitutive behaviour of reinforced concrete. In some damage models, during the loading/unloading process, a zero stress corresponds to a zero strain and the value of the damage is thus overestimated (Figure 1(b)). An elastic plastic relation is not valid

either, even with softening (see Figure 1(a)), as the unloading curve follows the elastic slope. A correct plastic-damage model should be capable of representing the softening behaviour; the damage law reproduces the decreasing of the elastic modulus, while the plasticity effect accounts for the irreversible strains (Figure 1(c)).

There are three ways to represent this behaviour (Simo and Ju, 1987):

(1) One of these ways, based on a plastic-damage coupled model, evaluates the damage and the plastic behaviours at the same time. The free energy can be expressed as the sum of elastic energy with the plastic energy, both of them influenced by the damage parameter

$$\Psi = \Psi^e(\varepsilon, d) + \Psi^p(q^p, d) \tag{39}$$

where d is the internal damage variable and q^p is the internal plastic variable.

(2) Another option is to assume the free energy to be the sum of the elastic energy with the plastic energy and one term dependent on damage. The result is that the dissipation energy is influenced by the damage parameter as the plasticity parameter

$$\Psi = \Psi^e(\varepsilon, d) + \Psi^p(q^p) + \Psi^d(q^d) \tag{40}$$

(3) The last option is to consider that damage and plasticity are uncoupled following their own laws independently; this way can be used when there are permanent deformations:

$$\Psi = \Psi^e(\varepsilon, d) + \Psi^p(q^p) \tag{41}$$

5.1 Uncoupled plastic-damage model
5.1.1 Thermodynamic references. As commented before, in the concrete of reinforced concrete elements, the damage effect modifies the constitutive plastic equation for small deformations by the degradation of the stiffness. A new constitutive equation is formulated without time variation of temperature for thermodynamically stable problems, using the following mathematical formulation for the free energy constituted by elastic and plastic terms (Oller, 2001):

$$\Psi(\mathbf{\Phi}^e, \mathbf{D}, q^p, q^d) = \Psi^e(\mathbf{\Phi}^e, \mathbf{D}, q^d) + \Psi^p(q^p) \tag{42}$$
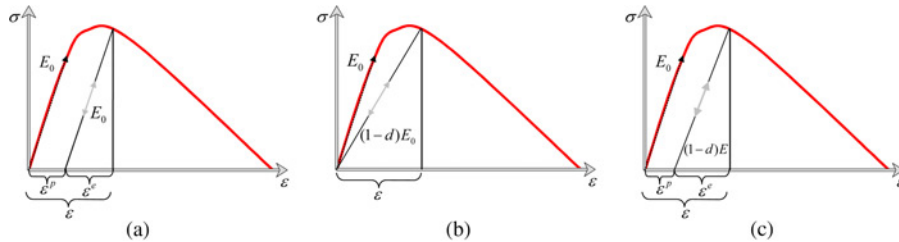

Figure 1.
Loading-unloading behaviour: simulated and experimental

Notes: (a) Plastic model, (b) damage model and (c) experimental behaviour

where $\mathbf{\Psi}^p$ is a plastic potential function and $\mathbf{\Psi}^e(\mathbf{\Phi}^e, \mathbf{D}, q^d)$ is the initial elastic stored energy. Additionally, q^p and q^d indicate the suitable set of internal (plastic and damage, respectively) variables and the elastic deformations $\mathbf{\Phi}^e$ is the free variable in the process.

For stable thermal state problems, the Clausius-Duhem dissipation inequality (Malvern, 1969) is valid and takes the form

$$\dot{\Xi} = \boldsymbol{M}_b \cdot \dot{\boldsymbol{\Phi}}_b - \dot{\Psi}_b \geq 0 \tag{43}$$

This inequality is valid for any loading-unloading stage. Taking the time derivative of Equation (42) and substituting into (43) the following equation is obtained for dissipation:

$$\dot{\Xi} = \left[\boldsymbol{M}_b - \frac{\partial \Psi_b}{\partial \boldsymbol{\Phi}_b^e} \right] \cdot \dot{\boldsymbol{\Phi}}_b + \frac{\partial \Psi_b}{\partial \boldsymbol{\Phi}_b^e} \cdot \dot{\boldsymbol{\Phi}}^p - \frac{\partial \Psi_b}{\partial \mathbf{D}^b} \cdot \dot{\mathbf{D}}^b - \frac{\partial \Psi_b}{\partial q^b} \cdot \dot{q}^p \geq 0 \tag{44}$$

In order to guarantee the unconditional fulfilment of the Clausius-Duhem inequality, the multiplier of $\dot{\boldsymbol{\Phi}}$ representing an arbitrary temporal variation of the free variable must be null. This condition provides the constitutive law of the damage problem

$$\left[\boldsymbol{M}_b - \frac{\partial \Psi_b}{\partial \boldsymbol{\Phi}_b^e} \right] = \mathbf{0}, \quad \forall \dot{\boldsymbol{\Phi}}_b \tag{45}$$

from where the final generalized stress of member can be defined as

$$\boldsymbol{M}_b = \frac{\partial \Psi_b}{\partial \boldsymbol{\Phi}_b^e} \tag{46}$$

Once imposed the condition $\boldsymbol{\Phi}_b^e = \boldsymbol{\Phi}_b - \boldsymbol{\Phi}_b^p$, the free energy for an elastic-plastic frame element with stiffness degradation can be written for small deformations as

$$\Psi_b(\boldsymbol{\Phi}_b^e, \mathbf{D}^b, q^p) = \frac{1}{2}(\boldsymbol{\Phi}_b - \boldsymbol{\Phi}_b^p) \cdot [\mathbf{S}_b^d(\mathbf{D}^b)] \cdot (\boldsymbol{\Phi}_b - \boldsymbol{\Phi}_b^p) + \Psi_b^p(q^p) \tag{47}$$

where the stiffness matrix of the damaged member $\mathbf{S}_b^d(\mathbf{D}_b)$ is the same matrix defined in (24). By replacing this last equation in (46) one arrives at the expression for plastic-damage analysis (Cipolina *et al.*, 1995; Flórez-López, 1993; Faleiro *et al.*, 2008):

$$\boldsymbol{M}_b = \mathbf{S}_b^d(\mathbf{D}^b) \cdot (\boldsymbol{\Phi}_b - \boldsymbol{\Phi}_b^p) \tag{48}$$

5.2 "Ad-hoc" homogenization of the RC cross-section to obtain the m_p and m_d limit moments

In this section, the classic homogenization concept is used to obtain the limit moments for the reinforced concrete members and for the constitutive models of plasticity and damage already presented in previous sections.

From experimental observations, it is well know that damage in concrete is a continuous process that initiates at very low levels of the applied loading, with an increasing amount of damage for increasing levels of strain. Conversely, the behaviour of the reinforcement steel is dominated by plasticity laws and only at very high load the damage materializes. Thus, for reinforced concrete structures, the plasticity is

physically associated to the flow of the reinforcement, while the damage indicates the cracking and rupture of the concrete. In the model described before, the developments are appropriate for bars composed of homogeneous materials. Now we introduce an approach in order to include the steel bars in the formulation.

A possible solution to combine different materials in an arbitrary cross-section of a beam would be the use of homogenization; the mentioned cross-section is subdivided in layers having assigned the corresponding characteristics of the material. In this way, for layers that contain steel, an elastic-plastic behaviour is assumed while, for concrete, damage with plasticity behaviour is considered. This idea has been simplified in this article, by assigning *a priori* the position within the cross-section of the concrete and steel layers together with their geometric quantities. In this way, a behaviour represented by one of the constitutive models detailed in previous sections is assigned to each layer. Thus, the homogenization manages the damage or plastic constitutive models and then makes the composition of the stress evolution over the cross-section of the reinforced concrete members. Then, the contributions of the materials that compound the cross-section are integrated to obtain the bending moments m_p (*plastic moment*) and m_d (*damage moment*) of the reinforced concrete beam. m_d indicates the beginning of the micro-crack in the cross-section due to the degradation (damage) of the concrete matrix.

Consider the classical, single reinforced, rectangular cross-section of width b and depth h' measured from the compression face to the centre of the steel bars, shown in Figure 2. The equilibrium of the horizontal forces requires that $(0.85f_c)ba = A_sf_y = T$, where T is the tensile steel resultant, f_y is the uniaxial yield strength of the bars and A_s is the combined cross-section area of all tensile steel bars. Thus,

$$a = \frac{A_sf_y}{0.85f_cb} \tag{49}$$

Since the distance from the resultant **C** of the compressive stresses in concrete to the tensile resultant T is $h' - (1/2)a$, the plastic moment is

$$m_p = A_sf_y\left(h' - \frac{1}{2}a\right) = A_sf_y\left(h' - \frac{1}{2}\frac{A_sf_y}{0.85f_cb}\right) \tag{50}$$

Equation (50) is valid only if the tensile steel yields before the compressed concrete crushes. For those cases where the longitudinal reinforcing steel bars are placed near the
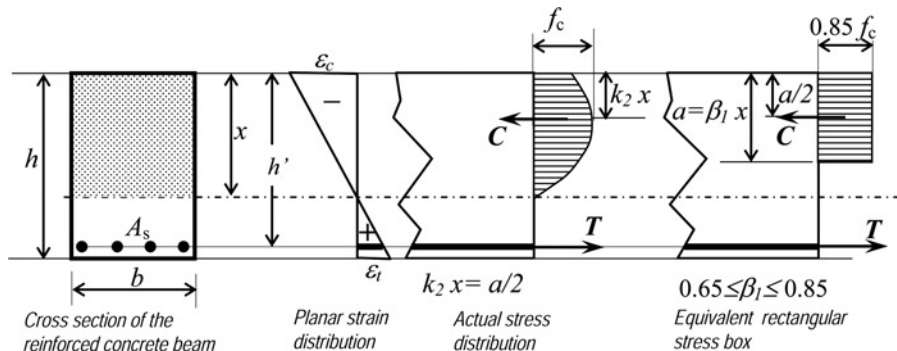
Figure 2.
Singly reinforced rectangular beam: cross-section and distributions of strains and stress

compressed face of the beams, Equation (50) can be rewritten as (Bazant and Jirásek, 1996)

$$m_p = 0.85 f_c ba\left(h' - \frac{1}{2}a\right) + A'_s f_y(h' - d') \tag{51}$$

where d' is the distance of the compression steel to the tensile face, A'_s is the compression steel cross-section area and

$$a = \frac{(A_s - A'_s)f_y}{0.85 f_c b} \tag{52}$$

In order to indicate the beginning of the cracking of the beam, we consider a damage bending moment m_d whose value is relatively small, usually 1/6 to 1/4 of the maximum service load (see Figure 3). This moment can be calculated from Equation (50) or (51), by setting the stress f_y at the tensile face equal to the so-called modulus of rupture (flexural strength) of concrete f_r (Bazant and Jirásek, 1996).

The plastic moment m_p will be used to determine the plastic limit behaviour of the beam, while the damage bending moment m_d will be used to determine its damage limit behaviour. Furthermore, the elastic modulus E will be calculated by the mixing theory (Car et $al.$, 2000), which supposes that all the materials have a perfect adherence to each other, leading to the following equivalent elastic modulus

$$E = (1 - \rho)E_c + \rho E_s \tag{53}$$

where E_c and E_s are the elastic modulus of the concrete and steel, respectively, while $\rho = A_s/b\,h'$ is the value of the steel ratio.

6. Global damage indices
6.1 Member damage index
The idea of the member damage index definition stemmed from a macroscale analogy with the continuous damage model definition. The starting point for its deduction is the assumption that we can express the plastic-damage free energy of a member $\Psi_b(\mathbf{\Phi}_b^e, \mathbf{D}^b, q^p) = \Psi_b^e(\mathbf{\Phi}_b^e, \mathbf{D}^b) + \Psi_b^p(q^p)$ of Equation (47) in function of the non-damaged free energy, Ψ^0, defined by Equation (25), as
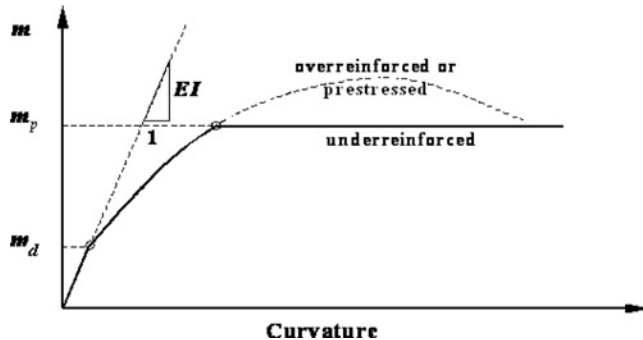

Figure 3.
Moment-curvature diagram for reinforced concrete beams failing by yielding of steel or by crushing of concrete

$$\Psi_b^e(\mathbf{\Phi}_b^e, \mathbf{D}^b) = (1 - D_M^b)\mathbf{\Psi}_b^0; \quad \begin{cases} \Psi_b^e(\mathbf{\Phi}_b^e, \mathbf{D}^b) = \dfrac{1}{2}\mathbf{\Phi}_b^e \cdot \mathbf{S}_b^d(\mathbf{D}^b) \cdot \mathbf{\Phi}_b^e \\ \Psi_b^0(\mathbf{\Phi}_b^e) = \dfrac{1}{2}\mathbf{\Phi}_b^e \cdot \mathbf{S}_b^0 \cdot \mathbf{\Phi}_b^e \end{cases} \tag{54}$$

where D_M^b is the member damage index. Solving (54) for D_M^b, we obtain

$$D_M^b = 1 - \frac{\Psi_b^e(\mathbf{\Phi}_b^e, \mathbf{D}^b)}{\Psi_b^0} \tag{55}$$

which is the expression of the damage index for the member of a frame. We can notice in Equation (55) that for those cases where only damage is considered, that is $\mathbf{\Phi}_b^p = 0$, we obtain that D_M^b indicates the evolution of the concentrated damage at the hinges. Otherwise, when we have only plasticity, that is $\mathbf{D}^b = 0$, D_M^b indicates the increment of the plasticity at the hinges.

6.2 Global damage index
The global damage index is defined as the sum of $\Psi_b^e(\mathbf{\Phi}_b^e, \mathbf{D}^b)$ divided by the sum of the non-damaged free energy Ψ_b^0

$$D_G = 1 - \frac{\displaystyle\sum_{b=1}^{3n} \Psi_b^e(\mathbf{\Phi}_b^e, \mathbf{D}^b)}{\displaystyle\sum_{b=1}^{3n} \Psi_b^0} = 1 - \frac{\displaystyle\sum_{b=1}^{3n} (\mathbf{\Phi}_b - \mathbf{\Phi}_b^p) \cdot \mathbf{S}_b^d(\mathbf{D}^b) \cdot (\mathbf{\Phi}_b - \mathbf{\Phi}_b^p)}{\displaystyle\sum_{b=1}^{3n} \mathbf{\Phi}_b^e : \mathbf{S}_b^0 : \mathbf{\Phi}_b^e} \tag{56}$$

where D_G is the global damage index. Replacing $M_b^0 = \mathbf{S}_b^e : \mathbf{\Phi}_b^e$, as well as $M_b = \mathbf{S}_b^d(\mathbf{D}^b) : (\mathbf{\Phi}_b - \mathbf{\Phi}_b^p)$, the following equation is obtained:

$$D_G = 1 - \frac{\displaystyle\sum_{b=1}^{3n\text{th}} \mathbf{\Phi}_b^e : M_b}{\displaystyle\sum_{b=1}^{3n\text{th}} \mathbf{\Phi}_b^e : M_b^0} \tag{57}$$

This global damage index is similar to that proposed by Flórez-López (1993) for FE analysis.

The global damage index, as well as the member damage index, is a basic tool for assessing the overall state of a structure. It gives a measure of the stiffness loss of a structure since the non-linear internal forces are influenced not only by the damage but also by the plasticity.

7. Numerical implementation of the plastic-damage model
The most important results obtained by using the proposed model are: deformations $\mathbf{\Phi}_b$, stresses $\mathbf{M}_b$, internal forces $\mathbf{F}_{int}$, plastic deformations $\mathbf{\Phi}_b^p$, the concentrated damage vector $\mathbf{D}$ of the structural members together with the global damage index of the structure and, if necessary, the remaining internal variables and their associated forces for each member of the structure.

These results are obtained by using the equilibrium equation (7) (quasi-static problems) together with the state law (48) in accordance with the internal variables evolution laws (16) and (18). Table I shows the implicit Newmark time integration scheme used for quasi-static problems.

Let us now focus our attention on the calculation of the member stresses and of the internal variables (Table I). The plastic and damage parameters can be calculated separately, as explained in section 5. This assumption comes from the observation that damage is linked to the concrete, while yielding is related with the steel. Therefore, the damage and the plastic evolution can be determined by Equations (29)-(36) for damage and by Equations (14)-(18) for the plastic behaviour.

Table II shows the procedure for determining the parameters.

8. Numerical examples

8.1 Validation example of the proposed numerical model

The model proposed in this article for reinforced concrete framed structures is also applicable to single material structures like steel frames. In this sense, the objective of this first example is to demonstrate the capability of the proposed model to analyse

---

A. First iteration (from time instant t to time instant $t + 1$)
- Update relevant matrices in the time $t + 1$

$$\mathbf{K}_t^{(1)} = \sum_{b=1}^{n\ elements} \mathbf{B}_b^T : \mathbf{S}_b^d(\mathbf{D}_b^{t-1}) : \mathbf{B}_b$$

- Compute:

$$\hat{\mathbf{F}}_{t+1}^{(1)} = \mathbf{F}_{ext} - \mathbf{K}_t^{(1)} \cdot \mathbf{U}_{t-1}; \quad \{\mathbf{D}\}_t^{(1)} = \{\mathbf{D}\}_{t-1}; \quad \{\boldsymbol{\Phi}^p\}_t^{(1)} = \{\boldsymbol{\Phi}^p\}_{t-1}$$

B. Loop over global convergence iterations: nth iteration
- Calculate the first approximations for the iteration n:

$$[\mathbf{J}] = -\left|\frac{\partial \hat{\mathbf{F}}_t^{(n)}}{\partial \mathbf{U}_t^{(n)}}\right|; \quad \Delta \mathbf{u}_t^{(n)} = \mathbf{J}^{-1} \cdot \hat{\mathbf{F}}_t^{(n)}; \quad \mathbf{U}_t^{(n)} = \mathbf{U}_t^{(n-1)} + \Delta \mathbf{u}_t^{(n)}$$

- Compute the member stresses and internal variables:

$$\{\boldsymbol{\Phi}_b\}_t^n = \mathbf{B}_b \cdot \mathbf{U}_t^n; \quad \{\mathbf{M}_b\}_t^n = [\mathbf{S}_b(\mathbf{D}_b)_t^n] : (\{\boldsymbol{\Phi}_b\}_t^n - \{\boldsymbol{\Phi}_b^p\}_t^n)$$

- Updates relevant matrices:

$$\{\mathbf{F}_{int}^D\}_t^{(n)} = \sum_{b=1}^{n\ elements} \mathbf{B}_b^T : \{\mathbf{M}_b\}_t^n; \quad \hat{\mathbf{F}}_t^{(n)} = \mathbf{F}_{ext} - \{\mathbf{F}_{int}^D\}_t^{(n)}$$

- If the residual forces norm $\|\hat{\mathbf{F}}_t^{(n)}\|/\|\mathbf{F}_{ext}(t)\| \leq TOL$, end of iterations and beginning of the computations in the next time step. If not, back to step 1 and proceed calculating

Table I.
Non-linear time integration scheme (Newton-Raphson)

I. For each b elements at nth iteration:
  (1) *Generalized deformations at the step:* $\{\mathbf{\Phi}_b\}_t^{(n)} = \mathbf{B}_b \cdot \mathbf{U}_t^{(n)}$.
  (2) *Verification of the evolution of the damage:*
    (i) Update of the internal variables: $\{\mathbf{D}_b\}_t^{(n)} = \{\mathbf{D}_b\}_t^{(n-1)}$; $\{\mathbf{r}_b\}_t^{(n)} = \{\mathbf{r}_b\}_t^{(n-1)}$.
    (ii) Determination of the undamaged energy norm vector: $\boldsymbol{\tau}_\Phi^b = \sqrt{\{\mathbf{\Phi}_b\}_t^{(n)} \cdot \mathbf{S}_b \cdot \{\mathbf{\Phi}_b\}_t^{(n)}}$
    (iii) Verification of the evolution of the damage: if $g(\tau_\Phi^b, (\mathbf{r}_b)_t^{(n)}) \leq 0$ No damage evolution $\rightarrow$ (3).
    (iv) Update of damage variable: $\{\mathbf{D}_b\}_t^{(n)} = G(\tau_\Phi^b)$.
    (v) Update of damage threshold: $\{\mathbf{r}_b\}_t^{(n)} = \{\tau_\Phi^b\}$.

  (3) *Verification of the evolution of the plastic variable:*
    (i) Determination of generalized effective "trial" stress and update of internal variables:

$$\{\Delta\mathbf{\Phi}_b^p\}_0 = \{\mathbf{\Phi}_b^p\}_t^{(n-1)}; \quad \{\Delta q^p\}_0 = \{q^p\}_t^{(n-1)}$$

    (ii) Plastic evolution $k = k + 1$:

$$\{\overline{\mathbf{M}}_b^{trial}\}_k = [\mathbf{S}_b] : (\{\mathbf{\Phi}_b\}_t^{(n)} - \{\Delta\mathbf{\Phi}_b^p\}_{k-1})$$

    (iii) Verification of flow conditions and determination of plastic multiplier

IF $\boxed{\begin{array}{l} (\dot{\lambda}_i^p)_k = 0 \ \ \text{if} \ [f_i]_{k-1} = \left[\dfrac{|m_i^{trial}|}{m_p(\phi_i^p)} + \left(\dfrac{n_i^{trial}}{n_p(\delta^p)}\right)^2 - \alpha\right]_{k-1} < 0 \ \ \text{or} \ (\lambda_i^p)_k \dot{f}_i]_{k-1} < 0 \\[4mm] (\dot{\lambda}_j^p)_k = 0 \ \ \text{if} \ [f_j]_{k-1} = \left[\dfrac{|m_j^{trial}|}{m_p(\phi_j^p)} + \left(\dfrac{n_j^{trial}}{n_p(\delta^p)}\right)^2 - \alpha\right]_{k-1} < 0 \ \ \text{or} \ (\lambda_j^p)_k \dot{f}_j]_{k-1} < 0 \end{array}}$ **No Plasticity** $\rightarrow$ **(4)**.

Otherwise: plasticity

    (iv) Update of plastic variables and of the generalized effective "trial" stress:

$$(\dot{\phi}_i^p)_k = (\dot{\lambda}_i^p)_k \left(\frac{\partial f_i}{\partial m_i}\right)_{k-1}; \ \ (\dot{\phi}_j^p)_k = (\dot{\lambda}_j^p)_k \left(\frac{\partial f_j}{\partial m_j}\right)_{k-1}; \ \ (\dot{\delta}^p)_k = (\dot{\lambda}_i^p)_k \left(\frac{\partial f_i}{\partial n}\right)_{k-1} + \dot{\lambda}_j^p \left(\frac{\partial f_j}{\partial n}\right)_{k-1}$$

$$(m_i)_k = (m_i^{trial})_{k-1} - (\dot{\lambda}_i^p)_k \cdot \mathbf{S}_b \cdot \left\{\frac{\partial f_i}{\partial m_i^{trial}}\right\}_{k-1}; \ \ (m_j^{trial})_k = (m_j^{trial})_{k-1} - (\dot{\lambda}_j^p)_k \cdot \mathbf{S}_b \cdot \left\{\frac{\partial f_j}{\partial m_j^{trial}}\right\}_{k-1}$$

$$(n)_k = (n^{trial})_{k-1} - (\dot{\delta}^p)_k \cdot \mathbf{S}_b \cdot \left(\left\{\frac{\partial f_i}{\partial n^{trial}}\right\}_{k-1} + \left\{\frac{\partial f_j}{\partial n^{trial}}\right\}_{k-1}\right)$$

    (v) Back to (3) (ii)
  (4) *End of the process of plastic correction*

$$\{\mathbf{\Phi}_b^p\}_t^{(n)} = \{\Delta\mathbf{\Phi}_b^p\}_k; \quad \{q^p\}_t^{(n)} = \{\Delta q^p\}_k$$

[1] (5) *Achievement of the final generalized stress on the step n:*

$$\{\mathbf{M}_b\}_t^{(n)} = [\mathbf{S}_b(\mathbf{D}_b)_t^{(n)}] : (\{\mathbf{\Phi}_b\}_t^{(n)} - \{\mathbf{\Phi}_b^p\}_t^{(n)})$$

[2] (6) *End of integration process of the constitutive equation.*

Table II.
Procedure to the
determinations of the
damage and plastic
parameters

such structures and, at the same time, to validate the proposed model and to evaluate the related concentrated damage and the global damage index of these types of structures. For this reason, we will compare the results obtained by means of the proposed non-linear frame analysis model with those obtained by using more refined FE models.

The analysed frame is 4 m high and 4 m wide and loaded with two point forces (Figure 4(a)). The columns have a 8.43×5.62 cm cross-section, the horizontal beam is 5.62 cm thick and 12.65 cm wide. Two FE models have been considered by Oller *et al.* (1996a, b); the first one used three-noded Timoshenko beams elements to represent the structure (see Figure 4(d)) and the second used 75 2D eight-noded quadrilateral elements (see Figure 4(e)). Three frame models have been considered. The first one used only three elements: one for the column and two for the beam (see Figure 4(a)). In the case of the second frame model, the column and the beam have been represented by ten elements (see Figure 4(c)). For the last frame model, the division in three-noded beams elements was adopted, which is described in Figure 4(d).

In the numerical analysis of the frame, the used plastic constitutive equation only takes into account the bending moments, while the lineal damage equation, proposed by Oller (2001), has been considered for determining the damage variable evolution, using in this case a fracture energy G_f equal to 250 N/m. In all cases, the elastic modulus $E = 2.1 \times 10^5$ MPa while for the frame analysis it was assumed that the ultimate moment $m_p = 45$ kN m for the beam and $m_p = 20$ kN m for the column. The material behaves in elasto-plastic way: once reached the elastic limit $f_y = 200$ MPa, it yields indefinitely at constant stress. Figure 5 shows the results of the evolution of the force vs the displacement in the left upper corner of the frame obtained for each model. It can be noticed that the results calculated with the proposed frame

Figure 4.
Geometry of the studied frame
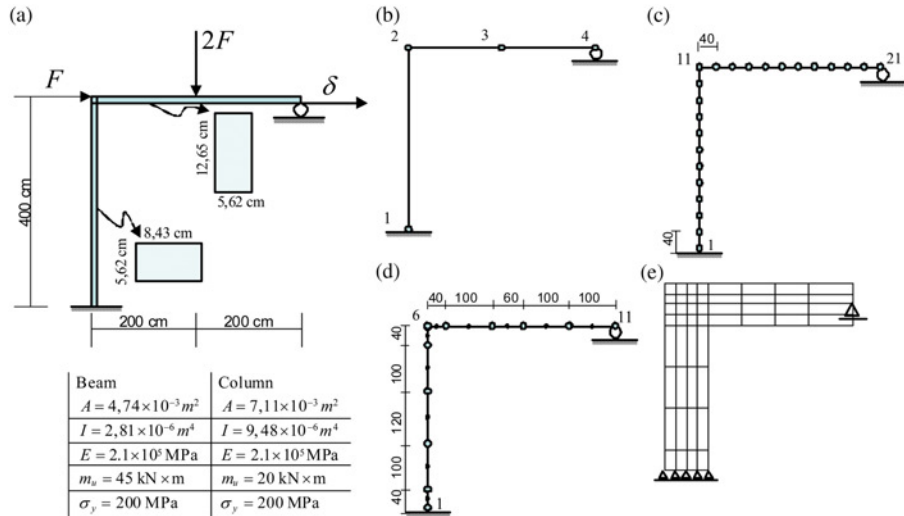
Notes: (a) Geometry and cross-section, (b) numeration of the nodes of the frame model with three elements, (c) numeration of the nodes of for the frame model with 20 elements, (d) FE mesh using Timoshenko three-noded beams elements and (e) FE mesh using 2D eight-noded quadrilateral elements

analysis model are in good agreement with the results obtained with the FE model. In this analysis, plasticity and damage were considered together.

The evolution of the moment at the column base is shown in Figure 6, where a comparison is made among the results obtained with the proposed method for different frame models. The evolution of the global damage index for each frame is shown in Figure 7. The concentrated damage at the base and the top of the columns of each frame has also been monitored, once it was clearly expected the structural failure due to the weakening of the column. Studying together these three graphs, we can analyse the behaviour of each frame.

The damage at the column base is less than the global damage index obtained for all cases (see Figure 7). The same curves are calculated for the frames modelled with 10 and 20 elements, obtaining the force-displacement relation (Figure 5), moment-displacement
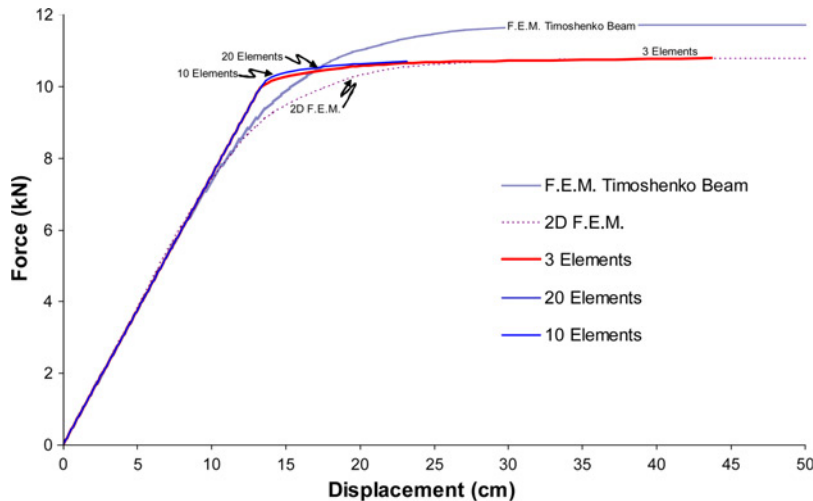
Figure 5.
Comparison of the force-displacement curve for FE results with the results obtained by using the proposed plastic-damage model
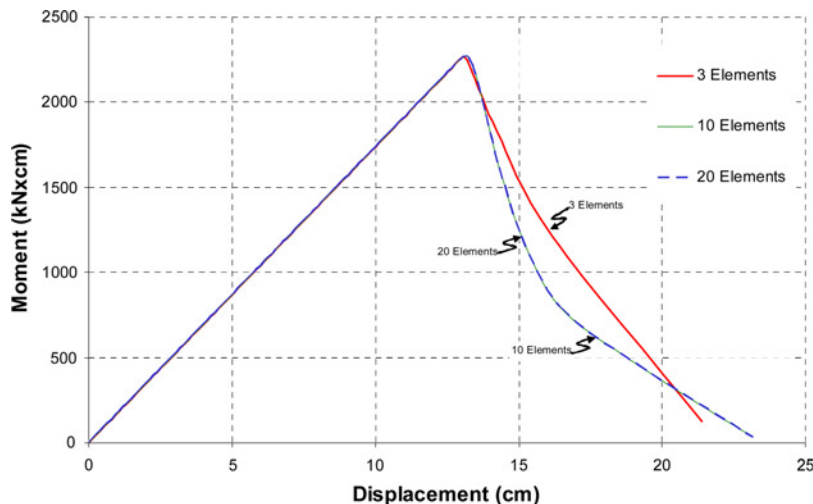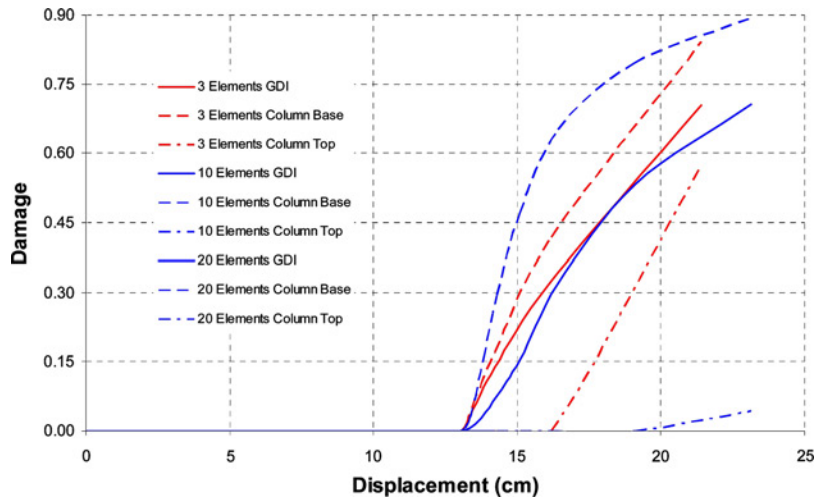

Figure 6.
Moment on the column base vs displacement at the left upper corner

relation (Figure 6), global damage index evolutions and evolutions of the damage of the columns (Figure 7).

Analysing the damage of the frame modelled with three elements, the beginning of the concentrated damage at the top of the column is closer to the beginning of the concentrated damage at its base, and both have almost the same final value. Meanwhile, for the frame with 10 and 20 elements, the damage at the top begins at very high loads while the damage at the base begins almost at the same instant when plasticity begins. In both frames, the final value obtained for the concentrated damage at the base is higher than the value obtained at the top of the column.

For the frame modelled with three elements, it can be seen clearly that the evolution of the global damage index is not related only to the concentrated damage evolution but also to the plasticity evolution at the hinges. We can also notice that for both the frames modelled with 10 and 20 elements, the global damage index rapidly reaches high values for low deformations, what implies that the concentrated damage has more influence on the structural collapse than the plastic hinges, that is, the structure has little tendency to deform. This can be because the column and the beams are composed by several elements, dispersing the effect of plasticity, while the damage is more concentrated at the base of the column. In conclusion, the behaviour of the structure can be influenced by the number of elements and, therefore, the results obtained are smaller than it is expected.

Using the plastic and local damage indices proposed in section 6, it can be observed in Figure 8 that the evolution of the plasticity and damage begins simultaneous at the same time in the frame modelled with three elements. However, the values obtained for plastic-damage index are higher than the values obtained for the local damage index. This occurred because plasticity is active and has influence in the behaviour of the structure.

Analysing the local and plastic-damage index of the frames modelled with 10 and 20 elements, it can be noticed that, the local and the plastic-damage indices are identical in
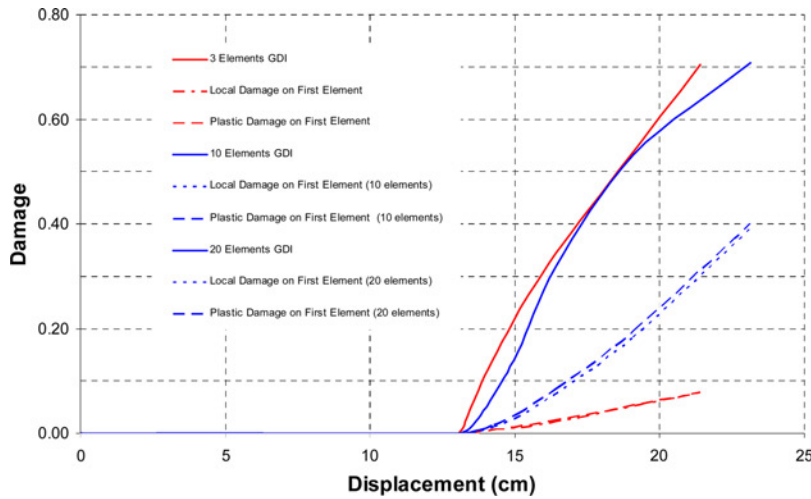
Figure 8.
Evolution of the GDI and
of the local and plastic
damage for the first
element

both cases. Similarly, the three elements frame model allows observing that the values of
the plastic-damage index are higher than the values obtained for the local damage index.

Analysing separately in Figure 9 the frame modelled with 20 elements, it can be
observed the evolution of the local and global damage indices. As expected, the higher
values of the plastic and local damage are obtained in the first element, located at the
base of the column, while the ninth and the tenth elements, at the top of the column,
show lower values of the plastic and local damage indices. The plastic-damage index at
the ninth element is indicative that plasticity occurs at both extremities of the tenth
element, contributing to the singularity of the stiffness matrix.

Apparently, the evolution of the global damage index describes only the evolution of
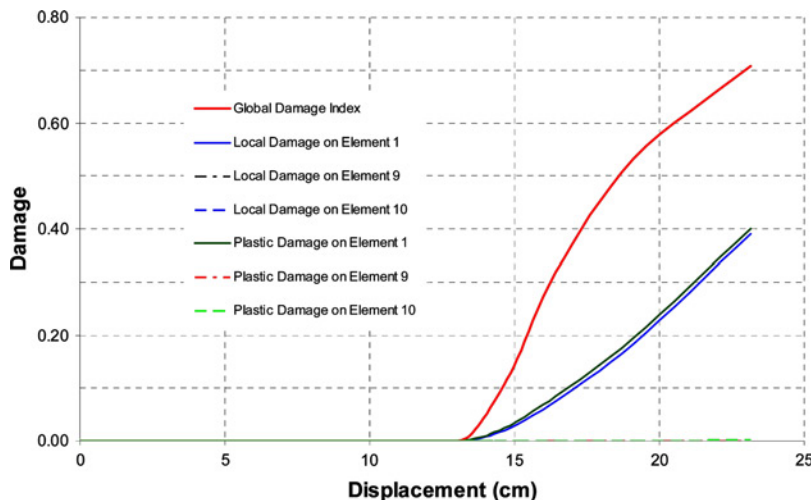the plasticity and the damage at the base of the column. This occurs because, in the

Figure 9.
Plastic and local damage
evolution on the elements
of the frame modelled
with 20 elements

frame modelled with 20 elements, we only have damage and plasticity at the base, and the structural stiffness is influenced by them. It is important to remember that the global damage index gives a measure of loss of structural stiffness, independent of how many members yield or are damaged.

8.2 Reinforced concrete framed structure

The objective of this example is to compare the results obtained by using the plastic-damage model described in section 5 with the results of a quasi-static laboratory test performed by Vecchio and Emara (1992) on a reinforced concrete frame. Barbat *et al.* (1997) have already performed a numerical simulation of the behaviour of the tested frame, but using a viscous damage model implemented in a FE program. A complete description of the geometrical and mechanical characteristics of the frame, as well as of the loads, is given in Figure 10.

The laboratory test consisted in applying a total axial load of 700 kN to each column and in maintaining this load in a force-controlled mode throughout the test, which thus produced their pre-compression. A horizontal force was afterwards applied on the beam of the second floor, in a displacement-controlled mode, until the ultimate capacity of the frame was achieved (Vecchio and Emara, 1992). In the numerical analysis of the frame, the plastic constitutive equation used only takes into account the bending moments, while the lineal damage equation proposed by Oller (2001) has been considered for determining the damage variable evolution, using in this case a fracture energy G_f equal to 250 N/m.
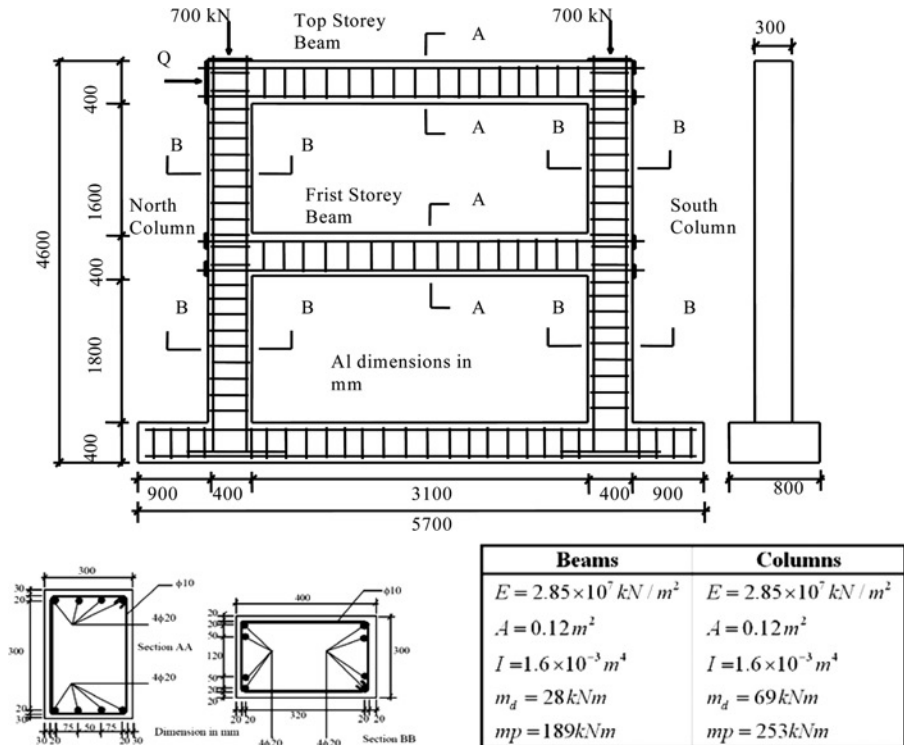

Figure 10.
Description of the geometrical and mechanical characteristics of the frame of Example 3

Beams	Columns
$E = 2.85 \times 10^7 \, kN/m^2$	$E = 2.85 \times 10^7 \, kN/m^2$
$A = 0.12 \, m^2$	$A = 0.12 \, m^2$
$I = 1.6 \times 10^{-3} \, m^4$	$I = 1.6 \times 10^{-3} \, m^4$
$m_d = 28 \, kNm$	$m_d = 69 \, kNm$
$mp = 189 \, kNm$	$mp = 253 \, kNm$

The curves of Figure 11 relate the horizontal forces and the displacements of the second floor beam and correspond to the load-unload laboratory test case and to the computer simulation using a viscous damage model proposed by Barbat *et al.* (1997) with the plastic-damage model proposed in the present work. The results are reasonably in agreement, taking into account the little computational effort required by the calculation with the proposed model. In the first load-unload cycle, marked by point 2 in Figure 11, the presence of residual deformations can be observed in the experimental curve, while in the numerical curve this does not occur. This is because the plastic-damage model still not reaches the plastic limit and the plastic deformations are assumed to occur only after the yielding of the reinforcement. Nevertheless, when one of the elements reaches the plastic limit, it is possible to observe the influence of the plastic hinge on the curve. This situation is noticeable by the residual deformations represented in the subsequently unload-load cycles, at points three and four in Figure 11. However, in the laboratory test, non-negligible permanent deformations occurred before this, probably because of the inelastic strains and cracking of the concrete.

Analysing the damage evolution at the first floor shown in Figure 12, and at the second floor shown in Figure 13, we can notice that the local damage begins in the first-storey beam, followed almost simultaneously by damage of the second-storey beam, and after that, the damage in the first floor columns occurs. Only after a considerable increase of the deformation, the damage begins in the second floor columns. This behaviour is in agreement with the evolution of the damage observed in the laboratory test.

The effect of the damage in the first-storey beam can also be detected in the force-displacement curve by point 1 in Figure 11, which indicates the end of the elastic phase of the structure. However, in the first unload process of the frame (point 2 in Figure 11) indicates that, at this moment, there is only damage in the frame model, aspect which is confirmed by the fact that the unload line returns to zero and all plastic-damage indices are null. At this point, as it was observed in the laboratory test, the damage occurs only at the first-storey beam, at the second-storey beam and at the columns of the first floor.

In the laboratory test, the structure looses stiffness because of the propagation of the cracks throughout all the members at the point 2. However, in the frame analysis, the
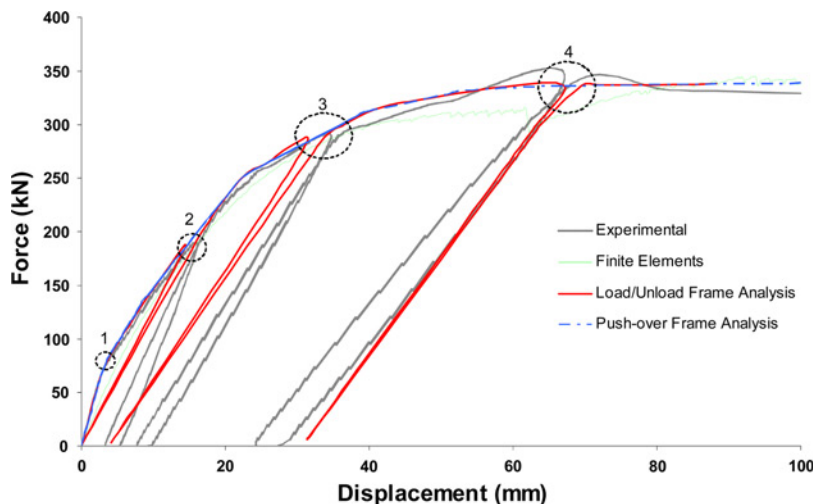

Figure 11.
Comparison of the experimental results with results obtained by using the frame analysis with the proposed plastic-damage model and a FE model
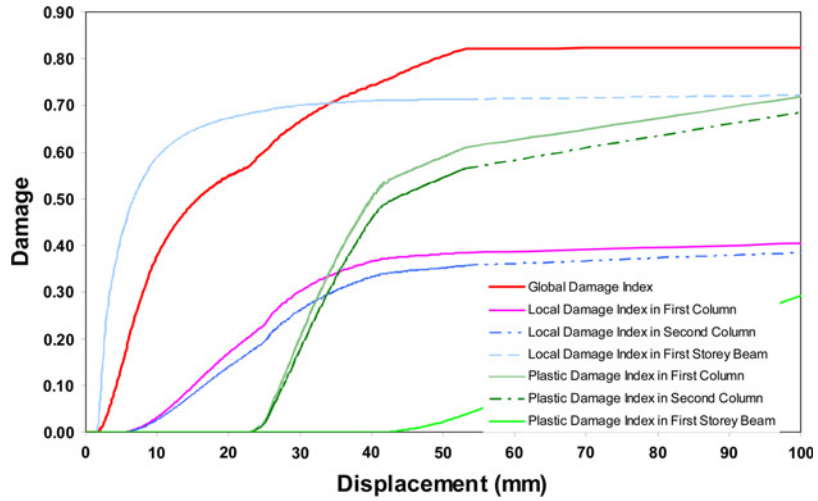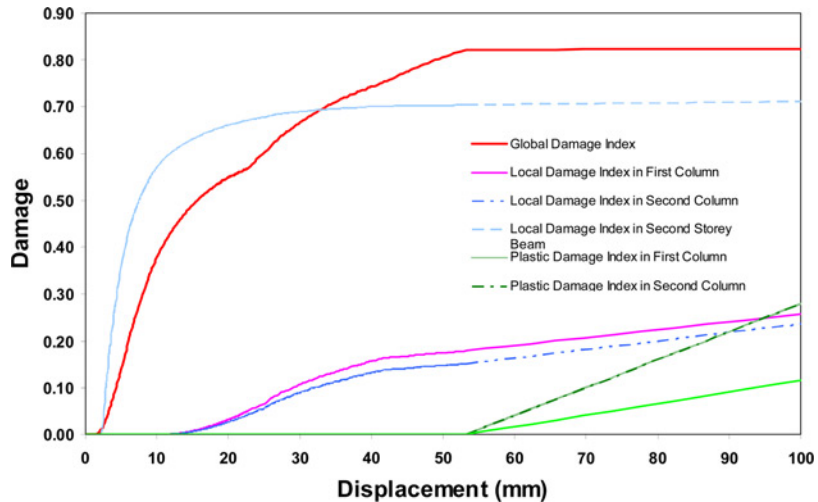
structure looses stiffness only when the plastic effect begins, for loads closer to point 3,
when yielding begins in the first floor at the base of both columns, indicated by the
increase of the plastic-damage indices for the first and second column at the first floor
in Figure 12.

In the laboratory test, the first yielding was detected at the bottom of the
longitudinal reinforcement at the end of the first-storey beam, followed by the yielding
at the base of both columns of the first floor. In contrast, as it can be observed in Figure
12 where the plastic damage increases, in the frame analysis the first yielding is
detected at the base of both columns of the first floor, followed by the yielding of the
first-storey beam. These differences in the sequence of yielding can be explained by the
fact that in the frame analysis the yielding of the end cross-section of the members is

sudden, and not gradual, or fibre-by-fibre, as observed in the first-storey beam in the laboratory test.

The occurrence of the perfect plastic hinge at the first-storey beam and at the base of the first and second columns of the first floor implies a change of the static configuration for the whole structure, resulting in a slight change of the local damage indices. This behaviour can also be observed by the change in curvature of the global damage index curve. Physically, this can be interpreted as the failure of the concrete in compression of the first floor columns and of the beams and the ensuing redistribution of the stresses towards the steel.

Meanwhile, in the frame analysis the plasticity in the second floor occurs only at the second-storey beam, as it can be seen in Figure 13. In this case, it can be observed by examining the plastic-damage index that the plasticity in the second-storey beam is sudden. At this point, the structure becomes unstable due to the development of many plastic hinges, increasing its deformation without an increase in load. Due to the increase of deformation, all plastic and damage indices, as well as the global damage, increases faster, generating a gap between the points where plasticity begins in the second-storey beam.

Anyway, in frame analysis, the plasticity in the first and second column of the second floor occurs only after a considerable increase of the deformations, by means of the formation of plastic hinges at the top of both columns.

9. Conclusions

A general framework for non-linear analysis of frames based on the continuum damage mechanics and plasticity theory has been developed. The plastic-damage model developed in this article assumes that plasticity and damage are uncoupled, have their own laws and that both are concentrated at ends of the frame members. Within this framework, many kinds of materials and loading conditions have been considered. Even the loading-unloading process has been simulated, and the values obtained provide satisfactory results when compared with laboratory tests, especially for reinforced concrete building.

The proposed model proves to be an effective tool for the numerical simulation of the collapse of frames. It could be a valuable alternative when other types of analyses, such as those based on multi-layer models, appear to be too expensive or impractical due to the size and complexity of the structure. The proposed model for reinforced concrete frames exhibited a very good precision confirmed by the examples included in the paper.

The global damage index has proved to be a powerful and precise tool for identifying the failure mechanism leading to failure of reinforced concrete frame structures. This index, together with the member and the concentrated damage indices, provides accurate quantitative measures for evaluating the state of any component of a damaged structure and of the overall structural behaviour. It is an excellent tool for the seismic damage evaluation, reliability and safety assessment of exiting structures and which can also be used in the evaluation of repair or retrofitting strategies.

References

Argyris, J.H., Boni, B. and Kleiber, M. (1982), "Finite element analysis of two and three – dimensional elasto-plastic frames – the natural approach", *Computer Methods in Applied Mechanics and Engineering*, Vol. 35, pp. 221-48.

Barbat, A.H., Oller, S., Oñate, E. and Hanganu, A. (1997), "Viscous damage model for Timoshenko beam structures", *International Journal of Solids Structures*, Vol. 34 No. 30, pp. 3953-76.

Bazant, Z.P. and Jirásek, M. (1996), "Softening-induced dynamic localization instability: seismic damage in frames", *Journal of Structural Engineering*, Vol. 122 No. 12, pp. 1149-58.

Car, E., Oller, S. and Oñate, E. (2000), "An anisotropic elastoplastic constitutive model for large strain analysis of fiber reinforced composite material", *Computer Methods in Applied Mechanics and Engineering*, Vol. 185 Nos. 2-4, pp. 245-77.

Cipolina, A., López Inojosa, A. and Flórez-López, J. (1995), "A simplified damage mechanics approach to nonlinear analysis of frames", *Computer and Structures*, Vol. 54 No. 6, pp. 1113-26.

Deierlein, G.G., Hajjar, J.F. and Kavinde, A. (2001), "Material nonlinear analysis of structures: a concentrated plasticity approach", S.E. Report 2001, Department of Civil Engineering, University of Minnesota.

Faleiro, J., Barbat, A.H. and Oller, S. (2005), "Plastic damage model for nonlinear reinforced concrete frame analysis", paper presented at VIII International Conference on Computational Plasticity (COMPLAS VIII), Barcelona.

Faleiro, J., Oller, S. and Barbat, A.H. (2008), "Plastic-damage seismic model for reinforced concrete frames", *Computers and Structures*, Vol. 86, pp. 581-97.

Flórez-López, J. (1993), "Modelos de daño concentrado para la simulación numérica del colapso de pórticos planos", *Revista Internacional de Métodos Numéricos para Cálculo y Diseño en Ingeniería*, Vol. 9 No. 2, pp. 123-39.

Flórez-López, J. (1995), "Simplified model of unilateral damage for RC frames", *Journal of Structural Engineering, ASCE*, Vol. 121 No. 12, pp. 1765-71.

Flórez-López, J. (1999), *Plasticidad y Fractura en Estructuras Aporticadas*, Monografía de Ingeniería Sísmica, Centro Internacional de Métodos Numéricos en Ingeniería (CIMNE), Barcelona.

Hanganu, A., Oñate, E. and Barbat, A.H. (2002), "A finite element methodology for local/global damage evaluation in civil engineering structures", *Computer and Structures*, Vol. 80, pp. 1667-87.

Kachanov, L.M. (1958), "On creep rupture time", *Proceedings of the Academy of Sciences of the USSR, Division of Engineering Science*, Vol. 8, pp. 26-31.

Lubliner, J., Oliver, J., Oller, S. and Oñate, E. (1989), "A plastic-damage model for concrete", *International Journal of Solids and Structures*, Vol. 25 No. 3, pp. 299-326.

Luccioni, B. and Oller, S. (1996), "Evaluación del daño sísmico en pórticos de hormigón armado", *Revista Internacional de Ingeniería de Estructuras*, Vol. 1 No. 1, pp. 1-16.

Luccioni, B., Oller, S. and Danesi, R. (1995), "Plastic damaged model for anisotropic materials", *Fourth Pan American Congress of Applied Mechanics (PACAM IV)*, Buenos Aires.

Malvern, L. (1969), *Introduction to the Mechanics of a Continuous Medium*, Prentice Hall, Englewood Cliffs, NJ.

Martinez, X., Oller, S., Rastellini, F. and Barbat, A.H. (2008), "A numerical procedure simulating RC structures reinforced with FRP using the serial/parallel mixing theory", *Computers and Structures*, Vol. 86, pp. 1604-18.

Mata, P., Barbat, A.H. and Oller, S. (2008a), "Two-scale approach for the nonlinear dynamic analysis of RC structures with local non-prismatic parts", *Engineering Structures*, Vol. 30, pp. 3667-80, doi:10.1016/j.engstruct.2008.06.011.

Mata, P., Barbat, A.H., Oller, S. and Boroschek, R. (2008b), "Constitutive and geometric nonlinear models for the seismic analysis of RC structures with energy dissipators", *Archives for Computational Methods in Engineering*, Vol. 15, pp. 489-539, doi: 10.1007/s11831-008-9024-z.

Mata, P., Oller, S. and Barbat, A.H. (2007a), "Static analysis of beam structures under nonlinear geometric and constitutive behaviour", *Computer Methods in Applied Mechanics and Engineering*, Vol. 196, pp. 4458-78.

Mata, P., Oller, S. and Barbat, A.H. (2007b), "Dynamic analysis of beam structures considering geometric and constitutive nonlinearity", *Computer Methods in Applied Mechanics and Engineering*, Vol. 197, pp. 857-78.

Oller, S. (2001), *Fractura Mecánica – Un Enfoque Global*, CIMNE, Barcelona.

Oller, S. and Barbat, A.H. (2005), "Moment-curvature damage model for bridges subjected to seismic loads", *Computer Methods in Applied Mechanics and Engineering*, Vol. 195 Nos. 33/36, pp. 4490-511.

Oller, S., Luccioni, B. and Barbat, A.H. (1996a), "Un método de evaluación del daño sísmico en estructuras de hormigón armado", *Revista Internacional de Métodos Numéricos para Cálculo y Diseño en Ingeniería*, Vol. 12 No. 2, pp. 215-38.

Oller, S., Luccioni, B. and Barbat, A.H. (1996b), "Un método de evaluación del daño sísmico en estructuras de hormigón armado", *Revista Internacional de Métodos Numéricos para el Cálculo y diseño en Ingeniería*, Vol. 12 No. 2, pp. 215-38.

Oñate, E., Oller, S., Oliver, J. and Lubliner, J. (1988), "A constitutive model of concrete based on incremental theory of plasticity", *Engineering Computation*, Vol. 5 No. 4, pp. 303-19.

Salomón, O., Oller, S. and Barbat, A.H. (1999), "Finite element analysis of base isolated buildings subjected to earthquake load", *International Journal of Numerical Methods in Engineering*, Vol. 46 No. 10, pp. 1741-61.

Simo, J.C. and Ju, J.W. (1987), "Stress and strain based continuum damage models-I. Formulation", *International Journal of Solids and Structure*, Vol. 23, pp. 821-40.

Vecchio, F.J. and Emara, M.B. (1992), "Shear deformations in reinforced concrete frames", *ACI Structural Journal*, Vol. 89 No. 1, pp. 45-6.

Corresponding author

S. Oller can be contacted at: sergio.oller@upc.edu